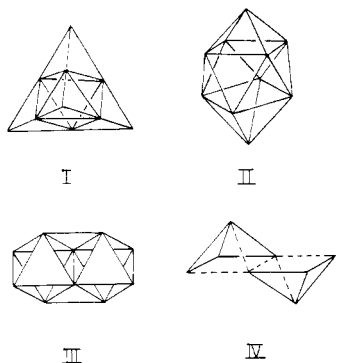


ligands appears at  $\delta$  457, a position that appears to be characteristic of  $\text{Ru}_6\text{C}$  cores.<sup>12</sup>

In comparison with the four previously characterized decanuclear clusters,  $\text{Ru}_{10}\text{C}_2(\text{CO})_{24}^{2-}$  is unique in both its structure and its electron count (138 valence electrons). The framework of  $\text{Os}_{10}\text{C}(\text{CO})_{24}^{2-13}$  is a tetracapped octahedron (see I) and its 134



valence electrons can be explained by Wade-Mingos rules.<sup>14,15</sup> In contrast  $\text{Rh}_{10}\text{S}(\text{CO})_{22}^{2-}$ ,<sup>16</sup>  $\text{Rh}_{10}\text{P}(\text{CO})_{22}^{3-}$ ,<sup>17</sup> and  $\text{Rh}_{10}\text{As}(\text{CO})_{22}^{3-18}$  each displays a bicapped square antiprism of metal atoms (see II) surrounding the non-metal atom and each has the 142 electrons predicted by Lauher.<sup>19</sup> Using a similar treatment, Ciani and Sironi<sup>20</sup> predicted 134 electrons for a ten-atom  $D_{2h}$  framework formed by two edge-fused octahedra plus apical-apical bonds (see III). The distorted framework observed for  $\text{Ru}_{10}\text{C}_2(\text{CO})_{24}^{2-}$  suggests that the "extra" four electrons present in the real compound may occupy metal-metal antibonding orbitals largely localized on the apical ruthenium atoms, thereby affecting the apical-apical interactions primarily and other bonds to the apical atoms to a lesser extent.

The electron count displayed by  $\text{Ru}_{10}\text{C}_2(\text{CO})_{24}^{2-}$  may be rationalized in the following way, which depends on the fact that a 74-electron square pyramid (e.g.,  $\text{Ru}_5\text{C}(\text{CO})_{15}$ ) has 18 electrons per metal atom, if localized M-M bonds are assumed, but an 86-electron octahedron (e.g.,  $\text{Ru}_6\text{C}(\text{CO})_{17}$ ) does not.<sup>15,19</sup> Removing two  $\text{Ru}(\text{CO})_2$  caps (maintaining inversion symmetry) leaves two square pyramids sharing a basal edge (see IV). This structure may be viewed as two discrete  $\text{Ru}_4\text{C}(\text{CO})_{10}^-$  "butterfly" units connected in a slipped fashion. The connection involves five Ru-Ru contacts between the subunits, which satisfies the 5-electron deficiency of each  $\text{Ru}_4\text{C}(\text{CO})_{10}^-$  moiety (cf.  $\text{Fe}_4\text{C}(\text{CO})_{12}^{2-}$ ).<sup>21</sup> Thus, the  $\text{Ru}_8\text{C}_2(\text{CO})_{20}^{2-}$  framework (114 electrons) is electron precise and adding the two capping  $\text{Ru}(\text{CO})_2$  units (each 12 electrons and providing no extra framework pairs<sup>15</sup>) gives the observed formulation.<sup>22</sup>

Dicarbide clusters have been observed previously only for cobalt and rhodium; two general classes have been characterized. In one class, represented by  $\text{Co}_{13}\text{C}_2(\text{CO})_{24}^{4-23}$  and  $\text{Rh}_{15}\text{C}_2(\text{CO})_{23}^{2-}$ ,<sup>24</sup> the carbon atoms are well separated and occupy two distinct cavities (trigonal prismatic for Co, octahedral for Rh) within the cluster framework. The second class, consisting of  $\text{Co}_{11}(\text{C}_2)(\text{CO})_{22}^{3-25}$  and  $\text{Rh}_{12}(\text{C}_2)(\text{CO})_{25}$ ,<sup>26</sup> populate a single cavity with a  $\text{C}_2$  unit. Although  $\text{Ru}_{10}\text{C}_2(\text{CO})_{24}^{2-}$  is a member of the first class, its more condensed structure brings the two carbon atoms in closer proximity. This suggests the possibility of conversion to the second class under appropriate conditions.

**Acknowledgment.** This research was supported at the University of Illinois by NSF Grant CHE 81-00140 (to J.R.S.) and at SUNY-Buffalo by NSF Grant CHE 80-23448 (to M.R.C.). FAB mass spectra were obtained at the University of Illinois by J. C. Cook, Jr., in part under a grant from the National Institute of General Medical Sciences (GM 27029).

**Supplementary Material Available:** Listings of atomic coordinates, bond lengths, and bond angles (13 pages). Ordering information is given on any current masthead page.

(23) Albano, V. G.; Braga, D.; Chini, P.; Ciani, G.; Martinengo, S. *J. Chem. Soc., Dalton Trans.* **1982**, 645-649.

(24) Albano, V. G.; Sansoni, M.; Chini, P.; Martinengo, S.; Strumolo, D. *J. Chem. Soc., Dalton Trans.* **1976**, 970-974.

(25) Albano, V. G.; Braga, D.; Ciani, G.; Martinengo, S. *J. Organomet. Chem.* **1981**, 213, 293-301.

(26) Albano, V. G.; Chini, P.; Martinengo, S.; Sansoni, M.; Strumolo, D. *J. Chem. Soc., Dalton Trans.* **1978**, 459-463.

## Reactions of Nucleophiles with $\alpha$ -Halo Ketones<sup>1</sup>

Glen A. Russell\* and Francisco Ros<sup>2</sup>

Department of Chemistry, Iowa State University  
Ames, Iowa 50011

Received July 30, 1982

Nucleophilic substitutions occurring by electron-transfer radical chain processes ( $\text{S}_{\text{RN}}1$ ) at the  $\alpha$ -C atoms of  $\alpha$ -nitro ketones and esters<sup>3</sup> or of  $\alpha$ -halomercury ketones<sup>4</sup> are recognized. Since the radical anion of  $\alpha$ -bromo-*p*-nitroacetophenone rapidly loses bromide ion,<sup>5</sup>  $\alpha$ -halo ketones are also candidates for  $\text{S}_{\text{RN}}1$  processes.

We have examined the reactions of sterically hindered  $\alpha$ -haloisobutyrophenones (1) with  $\text{Me}_2\text{C}=\text{NO}_2^-$  and found that with *p*-nitro or *p*-cyano substituents competing ionic and free-radical substitution processes lead to different products. However, since the free radical process is not observed in the reaction of a variety

(12) The value observed for  $(\text{CH}_3\text{CN})_2\text{Cu}_2\text{Ru}_6\text{C}(\text{CO})_{16}$  is  $\delta$  458.<sup>10</sup> The shift reported<sup>8</sup> for  $\text{Ru}_6\text{C}(\text{CO})_{16}^{2-}$  has been redetermined as  $\delta$  459; Bradley, J. S., personal communication.

(13) Jackson, P. F.; Johnson, B. F. G.; Lewis, J.; McPartlin, M.; Nelson, W. J. *H. J. Chem. Soc., Chem. Commun.* **1980**, 224-226.

(14) Wade, K. *Adv. Inorg. Chem. Radiochem.* **1976**, 18, 1-66.

(15) Mingos, D. M. P.; Forsyth, M. I. *J. Chem. Soc., Dalton Trans.* **1977**, 610-616 and references therein.

(16) Ciani, G.; Garlaschelli, L.; Sironi, A.; Martinengo, S. *J. Chem. Soc., Chem. Commun.* **1981**, 563-565.

(17) Vidal, J. L.; Walker, W. E.; Schoening, R. C. *Inorg. Chem.* **1981**, 20, 238-242.

(18) Vidal, J. L. *Inorg. Chem.* **1981**, 20, 243-249.

(19) Lauher, J. W. *J. Am. Chem. Soc.* **1978**, 100, 5305-5315.

(20) Ciani, G.; Sironi, A. *J. Organomet. Chem.* **1980**, 197, 233-248.

(21) Davis, J. H.; Beno, M. A.; Williams, J. M.; Zimmie, J.; Tachikawa, M.; Muettterties, E. L. *Proc. Natl. Acad. Sci. U.S.A.* **1981**, 78, 668-671.

(22) If the  $\text{Ru}_{10}$  cluster is divided into two  $\text{Ru}_5\text{C}(\text{CO})_{12}^-$  subunits, each subunit is five electrons deficient, but there are seven Ru-Ru contacts. However, an 86-electron octahedral complex has formally only 11 M-M bonds ( $108 - 86 = 22$ ) even though there are 12 M-M contacts in the octahedral frame.<sup>15</sup> (Note that the equivalent geometry for 86 electrons, a capped square pyramid, clearly has only 11 M-M bonds.<sup>19</sup>) Thus, if in joining the  $\text{Ru}_5\text{C}$  subunits, one of the Ru-Ru contacts per octahedron formed is not counted as bonding, the five-electron deficiency per subunit is satisfied by five Ru-Ru bonds.

(1) Electron transfer processes. Part 32. This work was supported by Grants CHE-7823866 and CHE-8119343 from the National Science Foundation.

(2) Postdoctoral Fellow of the Consejo Superior de Investigaciones Científicas de España, 1979-1981.

(3) Kornblum, N.; Boyd, S. D.; Stuchal, F. W. *J. Am. Chem. Soc.* **1970**, 92, 5783. Kornblum, N.; Boyd, S. D. *Ibid.* **1970**, 92, 5784. Russell, G. A.; Norris, R. K.; Panek, E. J. *Ibid.* **1971**, 93, 5839.

(4) Russell, G. A.; Hershberger, J.; Owens, K. *J. Am. Chem. Soc.* **1979**, 101, 1312.

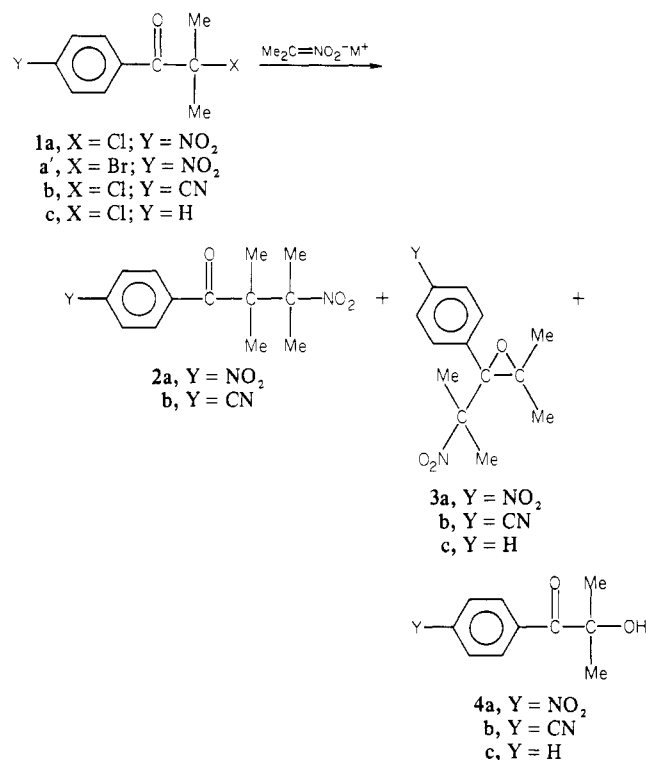
(5) Behar, D.; Neta, P. *J. Phys. Chem.* **1981**, 85, 690.

Table I. Reaction of  $p$ -YC<sub>6</sub>H<sub>4</sub>COCMe<sub>2</sub>X (1) with Me<sub>2</sub>C=NO<sub>2</sub><sup>-</sup>M<sup>+</sup> in Me<sub>2</sub>SO<sup>a</sup>

X	Y	M <sup>+</sup>	conditions <sup>b</sup>	time, min	yield, % <sup>c</sup>			
					2	3	4	1
Cl	NO <sub>2</sub>	Li <sup>+</sup>	$h\nu$	80	38	7	36	14
		K <sup>+</sup>	$h\nu$	80	41 (36)	16 (6)	32 (26)	6
		K <sup>+</sup>	dark	80	29	19	36	7
		K <sup>+</sup>	$h\nu$ , 10 mol % $p$ -DNB	45	28	16	31	20
		K <sup>+</sup>	$h\nu$ , 10 mol % (Me <sub>3</sub> C) <sub>2</sub> NO <sup>•</sup>	80	0	18	69	6
		K <sup>+</sup> , 18-crown-6	$h\nu$	80	77	10	10	0
	Br	Li <sup>+</sup>	$h\nu$	45	19	45	24	0
		K <sup>+</sup>	$h\nu$	15	8 (6)	62 (45)	4 (1)	0
		K <sup>+</sup>	$h\nu$ , 20 mol % (Me <sub>3</sub> C) <sub>2</sub> NO <sup>•</sup>	15	0	61	5	6
		K <sup>+</sup> , 18-crown-6	$h\nu$	45	51	28	4	0
		K <sup>+</sup> , 18-crown-6	dark	45	40	28	11	4
		K <sup>+</sup> , 18-crown-6	$h\nu$ , 20 mol % $p$ -DNB	45	27	48	5	6
		K <sup>+</sup> , 18-crown-6	$h\nu$ , 20 mol % (Me <sub>3</sub> C) <sub>2</sub> NO <sup>•</sup>	45	0	78	6	4
		K <sup>+</sup>	$h\nu$	60	51 (40)	12	18	0
		K <sup>+</sup>	dark	60	9	19	48	5
		K <sup>+</sup>	$h\nu$ , 15 mol % $p$ -DNB	60	7	18	32	23
Cl	CN	K <sup>+</sup>	$h\nu$ , 15 mol % (Me <sub>3</sub> C) <sub>2</sub> NO <sup>•</sup>	60	0	21 (14)	49 (39)	13
		K <sup>+</sup> , 18-crown-6	$h\nu$	60	69	5	12	0

<sup>a</sup> Standard conditions: the  $\alpha$ -halo ketone (1 mmol) in Me<sub>2</sub>SO was added with stirring under N<sub>2</sub> to Me<sub>2</sub>C=NO<sub>2</sub>M in Me<sub>2</sub>SO, prepared in situ from Me<sub>3</sub>COM, or Me<sub>3</sub>COK/18-crown-6 (1/1) (1.05 mmol) and Me<sub>2</sub>CHNO<sub>2</sub> (1.05 mmol) to give solution with [Li<sup>+</sup>] = [K<sup>+</sup>, 18-C-6] = 0.1 M; [K<sup>+</sup>] = 0.3 M (Me<sub>2</sub>C=NO<sub>2</sub>K was initially insoluble in Me<sub>2</sub>SO). <sup>b</sup>  $h\nu$ : irradiation with a 300-W sunlamp at ca. 50 cm. Dark: flask was wrapped with aluminum foil. <sup>c</sup> Crude yields by <sup>1</sup>H NMR analysis; numbers in parentheses represent yields of pure isolated products by TLC (silica gel; C<sub>6</sub>H<sub>6</sub>-ethyl acetate); all products gave satisfactory elemental analyses and <sup>1</sup>H NMR, IR, and mass spectral data.

Scheme I



of nucleophiles with the unsubstituted  $\alpha$ -chloroisobutyrophenone, we conclude that substitution in  $\alpha$ -halo ketones by an electron-transfer mechanism is a process of limited scope even when S<sub>N</sub>2 substitution is sterically hindered.

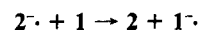
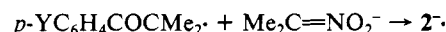
The reactions of 1a, 1a', or 1b with Me<sub>2</sub>C=NO<sub>2</sub><sup>-</sup> in Me<sub>2</sub>SO gave the  $\beta$ -nitro ketones 2, the oxiranes 3, and the  $\alpha$ -hydroxy ketones 4 (Scheme I), while 1c gave only 3c (60%) and 4c (12%). Table I summarizes the products from the reactions of 1a,b as a function of irradiation, the presence of free-radical scavengers, and the nature of the cation. The yields of the  $\beta$ -nitro ketones are higher with sunlamp irradiation than in the dark while 10–20 mol % of  $p$ -dinitrobenzene ( $p$ -DNB) or ( $t$ -Bu)<sub>2</sub>NO<sup>•</sup> caused partial or complete inhibition of their formation. The yields of the ox-

iranes 3 and the  $\alpha$ -hydroxy ketones 4 were not decreased in the dark or in the presence of the scavengers, their total yields increasing at the expense of 2. Complexation of the counterion of Me<sub>2</sub>C=NO<sub>2</sub><sup>-</sup>M<sup>+</sup> increased the yield of the  $\beta$ -nitro ketones. For example, the yield of 2a was increased from 41% to 77% by the presence of 18-crown-6 (K<sup>+</sup>, Me<sub>2</sub>SO).

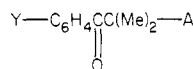
The formation of 2a and 2b is thus formulated as an S<sub>RN</sub>1 reaction (Scheme II).<sup>6</sup> The formation of 3 apparently involves

Scheme II

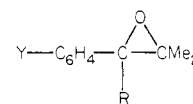
S<sub>RN</sub>1 mechanism (Y = O<sub>2</sub>N, CN)



nucleophilic attack by the carbon atom of Me<sub>2</sub>C=NO<sub>2</sub><sup>-</sup> at the carbonyl carbon of 1 followed by S<sub>N</sub>i displacement of halogen by the carbonyl oxygen atom. The  $\alpha$ -hydroxy ketones (4) may arise by O-attack of Me<sub>2</sub>C=NO<sub>2</sub><sup>-</sup> at either the  $\alpha$  or carbonyl carbon atoms of 1 to form nitronic esters, which decomposed during the reaction or upon workup.<sup>7</sup>



- 5a, Y =  $p$ -NO<sub>2</sub>; A = (EtO<sub>2</sub>C)<sub>2</sub>CH  
 5b, Y =  $p$ -NO<sub>2</sub>; A = (EtO<sub>2</sub>C)<sub>2</sub>CMe  
 5c, Y =  $p$ -NO<sub>2</sub>; A = C<sub>6</sub>H<sub>5</sub>S  
 5d, Y =  $p$ -NO<sub>2</sub>; A = C<sub>6</sub>H<sub>5</sub>SO<sub>2</sub>  
 5e, Y = H; A = C<sub>6</sub>H<sub>5</sub>S  
 5f, Y = H; A = C<sub>6</sub>H<sub>5</sub>SO<sub>2</sub>



- 6, Y =  $p$ -NO<sub>2</sub> or H;  
 R = C<sub>6</sub>H<sub>5</sub>C≡C- or  
 $n$ -C<sub>3</sub>H<sub>7</sub>C≡C-

(6) Russell, G. A. *Pure Appl. Chem.* **1971**, 23, 67. Kornblum, N. *Ibid.* **1971**, 23, 81; *Angew. Chem., Int. Ed. Engl.* **1975**, 14, 734. Bunnett, J. F. *Acc. Chem. Res.* **1978**, 11, 413.

(7) Attack of Me<sub>2</sub>C=NO<sub>2</sub><sup>-</sup> on the oxirane ring of 3 does not appear to be the source of 4 although this is a recognized reaction: Bachman, G. B.; Hokama, T. *J. Am. Chem. Soc.* **1959**, 81, 4223. Reaction of 3a with Me<sub>2</sub>C=NO<sub>2</sub><sup>-</sup>Li<sup>+</sup> under the reaction conditions of Table I failed to yield 4a, and the oxirane was recovered.

Other anions that react with **1a** by the  $S_{RN}1$  process are  $(EtO_2C)_2CR^-$  ( $R = H, Me$ ),  $PhS^-$ , and  $PhSO_2^-$ . With the malonate anions in  $Me_2SO$  only the  $S_{RN}1$  process was observed to yield **5a** (49%) and **5b** (62%), whose formation was completely inhibited by 10 mol %  $(t-Bu)_2NO$ . With **1c** alkylation was not observed with  $(EtO_2C)_2CMe^-$  and **4c** was the major product (62%).  $PhS^-$  and  $PhSO_2^-$  with **1a** gave **5c** and **5d** by competing  $S_{RN}1$  and ionic processes (the nitroxide retarded the photostimulated but not the dark reactions). Only ionic substitution was observed with **1c** to give **5e** and **5f**.  $PhC\equiv CLi$  or  $n-C_3H_7C\equiv CLi$  reacted (THF,  $-60^\circ C$ ) with **1a** or **1c** to give the oxiranes **6** in nearly quantitative yields, whereas  $(EtO)_2PO^-$  or  $(EtO)_2PS^-$  reacted with **1a** or **1c** in a process unaffected by irradiation or free-radical scavengers to give the known enol phosphates<sup>8</sup> and thiophosphates in a Perkow-type reaction.<sup>9,10</sup>

(8) Borowitz, I. J.; Anshel, M.; Firstenberg, S. *J. Org. Chem.* **1967**, 32, 1723.

(9) Lichtenthaler, F. W. *Chem. Rev.* **1961**, 61, 607.

(10) From **1c** the epoxy phosphonates (**5**,  $Y = H, A = (EtO)_2P(=O)$  and  $(EtO)_2P(=S)$ ) were also formed in  $Me_2SO$  or  $EtOH$ . The formation of both enol phosphates and epoxy phosphonates in the Michaelis-Becker reaction of  $\alpha$ -halo ketones is a known process.<sup>9</sup>

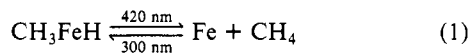
## Photoinduced Reductive Elimination of Iron Atoms and Methane from $CH_3FeH$

Geoffrey A. Ozin\* and John G. McCaffrey

Lash Miller Chemical Laboratories, University of Toronto  
Toronto, Ontario, Canada M5S 1A1

Received August 3, 1982

In this communication we report on a novel photoreversible reductive elimination/oxidative addition reaction (1)



in the  $Fe/CH_4$  system operating on a single iron atom site at 10–12 K and induced by 420- and 300-nm narrow-band irradiation, respectively.

Narrow-band irradiation into the intense 300-nm ( $3d^7 4p^1$ ,  $^5D_4 \leftarrow 3d^6 4s^2$ ,  $^5D_4$ ) atomic resonance line of Fe atoms<sup>1</sup> in  $CH_4$  under high dispersion ( $1/10^4$ ) conditions at 12 K caused rapid bleaching of all Fe atom bands with concomitant growth of a weak, broad absorption around 415–420 nm (Figure 1A–C). The corresponding infrared experiments (Figure 2) clearly demonstrated the production of the  $CH_3FeH$  insertion product absorbing strongly at 2921, 2888, 2869, 1650, 1148, 1145, 547, 544, 519, 300, 293  $cm^{-1}$ , which aside from slightly better resolution (see later) is in accord with the original observations of Billups et al.<sup>2</sup> The presence of a single intense  $\nu_{FeH}$  and three  $\nu_{CH}$  modes in the

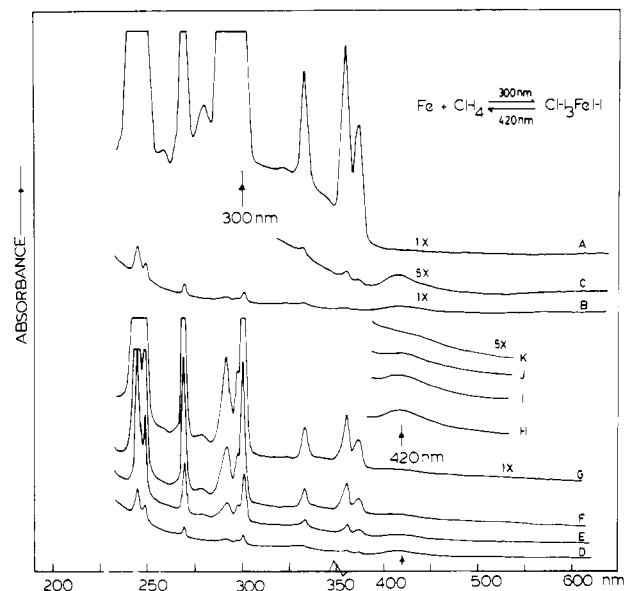


**Figure 1.** UV-visible spectra: (A) of Fe atoms isolated in solid  $CH_4$  ( $1/10^4$ ) at 10–12 K; (B) following 30 min of 300-nm photolysis (Oriol 450-W Xe lamp, Oriol monochromator 20-nm band pass, 10-cm water cell, intensity at the sample  $85 \mu W cm^{-2}$ ); (C) 5 $\times$  ordinate expansion of B in the 300–600-nm region; (D–G) samples similar to B at 0, 2, 7, and 12 min of 420-nm photolysis (intensity at the sample  $175 \mu W cm^{-2}$ ); (H–K) 5 $\times$  ordinate expansion of D–G in the 370–540-nm region.

iron-hydrogen and -methyl stretching regions, respectively, together argue in favor of a  $CH_3FeH$  rather than a  $CH_2FeH_2$  formulation for the  $Fe/CH_4$  300-nm photoproduct.

The thermal reactivity of Fe atoms with respect to  $CH_4$  was also examined in the accessible cryogenic range 10–50 K. Up to the temperature that the methane actually sublimed away from the sample window (around 50 K), no new infrared or optical bands, ascribable to an Fe atom- $CH_4$  reaction product, were ever observed.

Let us now focus attention on the 415–420-nm photoreactivity of the  $CH_3FeH$  insertion product, generated from 300-nm excitation of Fe atoms under rigorously monatomic conditions (Figure 1B,C). The outcome of these irradiations were probed by UV-visible and infrared spectroscopy. Both experiments showed the monotonic bleaching of the  $CH_3FeH$  absorptions with 420-nm irradiation time (Figure 1D–K). Especially noteworthy was the concurrent and rapid generation of atomic iron, clearly seen by the steady growth of the atomic resonance lines in the optical spectrum (Figure 1D–G). Infrared bands characteristic of new photoproducts were not observed at any time during the photoannihilation of  $CH_3FeH$ . The 420-nm photoproduction of Fe atoms from  $CH_3FeH$  is found to be highly efficient, and essentially quantitative, in terms of the ability to fully recover the Fe atoms consumed in the original 300-nm photogeneration of  $CH_3FeH$ . Furthermore, the atomic Fe produced in this photo-fragmentation process is identical in form (Figure 1D–G) with the originally deposited Fe atoms and moreover can be readily back-converted to  $CH_3FeH$  by further 300-nm excitation. These observations confirm that the photogenerated Fe atoms are not trapped in a special matrix site and/or in a different electronic state following their ejection from  $CH_3FeH$ .

Some information pertaining to the geometry of the ground electronic state of  $CH_3FeH$  can be derived from infrared spectroscopy. For  $CH_3FeH$  generated by 300-nm photoexcitation of Fe atoms in solid  $CH_4$ , one finds (Figure 2B) that the vibrational modes of  $CH_3FeH$  observed in the range 4000–250  $cm^{-1}$  are comprised of two types, those arising from symmetrical stretching and bending motions of CH, FeH, and FeC bonds and those

(1) Carstens, D. H. W.; Brashear, W.; Eslinger, D. R.; Gruen, D. M. *Appl. Spectrosc.* **1972**, 26, 184. Moore, C. *Natl. Bur. Stand. (U.S.) Circ.* 1949, Vol. I, 467; 1952, Vol. II; 1958, Vol. III.

(2) Billups, W. E.; Margrave, J. L.; Hauge, R. H. *J. Am. Chem. Soc.* **1980**, 102, 7393.